Single-Channel Neyman-Pearson Detection of Impulses in Tainter Valve Machinery Systems

LIN SUN, JOEY REED, DREW BARNETT, MICHAEL D. TODD, BRIAN EICK and CAROLYN ORTIZ

ABSTRACT

Unexpected mechanical failures in lock fill/empty Tainter valves can significantly disrupt waterway traffic. Accurate diagnosis and prognosis of fault mechanisms are essential for timely interventions by operations and maintenance teams. To support this, an in-service lock operated by the U.S. Army Corps of Engineers was instrumented with a comprehensive sensor suite—including accelerometers, strain gauges, inclinometers, thermocouples, and electrical current transformers—spanning the entire drive system from the motor to the final gear shaft. Data were collected during valve opening and closing operations using an event-driven approach. Notably, impulses were observed in the accelerometer signal at the sector gear during valve opening, coinciding with anomalies in the sector gear inclinometer data. To detect these impulses, a single-channel binary hypothesis testing framework based on the Neyman-Pearson theorem was implemented, modeling the signal as either zero-mean Gaussian noise or a non-zero mean Gaussian distribution with deterministic impulse magnitude incorporated. To address signal non-stationarity, an optimal sliding window size was selected to maintain stationarity and statistical reliability. Results from the Neyman-Pearson detection model are discussed, offering valuable insights into the operational health of the Tainter valve system and supporting the development of more robust diagnostic tools for lock infrastructure.

INTRODUCTION

Reliable mechanical health monitoring is vital for the safety and performance of engineering systems, allowing early anomaly detection and enabling predictive maintenance [1]. Recent advances in smart sensors have transformed data collection and real-time fault prevention [2]. Still, detecting anomalies remains difficult due to high data dimensionality, noise, uncertainties, and the challenge of separating normal behavior from true faults [3–5]. Hypothesis testing and detection theory play a key role in identifying faults based on system measurements, offering a probabilistic framework to locate and assess anomalies while accounting for real-world variability.

Tainter valves are key components in lock systems on inland riverways, regulating water depth in the lock chamber via culverts at each end. Poor maintenance can lead to structural failure and disrupt operations [6]. In the U.S., many Tainter valves are aging, facing wear, corrosion, and fatigue that threaten their integrity and performance [7]. Beyond structural concerns, failure of the valve-operating equipment can halt lock operations and severely impact the economic interests tied to inland navigation. Addressing these risks is essential to ensure the safety and efficiency of aging infrastructure.

Lin Sun, Department of Structural Engineering, University of California San Diego, 9500 Gilman Drive La Jolla, CA 92093, U.S.A.
Joey Reed, Elintrix, 621 South Andreasen Dr, Suite E, Escondido, CA 92029, U.S.A. Drew Barnett, Elintrix, 621 South Andreasen Dr, Suite E, Escondido, CA 92029, U.S.A.
Michael D. Todd, Department of Structural Engineering, University of California San Diego, 9500 Gilman Drive, La Jolla, CA 92093, U.S.A.
Brian Eick, Construction Engineering Research Laboratory, Engineer Research and Development Center, 2902 Newmark Drive, Champaign, IL 61822, U.S.A.
Carolyn Ortiz, Construction Engineering Research Laboratory, Engineer Research and Development Center, 2902 Newmark Drive, Champaign, IL 61822, U.S.A.

Anomaly detection methods have been applied across various domains and are generally categorized by how they isolate target signals in measured data—such as time-domain, frequency-domain, time-frequency domain, and singularity (Holder exponent) approaches [8]. Wee et al. [9] developed a CWT-based peak detection method for low signal-to-noise ratio (SNR) signals with shifting baselines. An et al. [10] proposed an acoustic signal-based pipeline leak detection algorithm using CFAR techniques, achieving improved performance with optimized parameters. Robertson et al. [11] applied the Holder exponent to detect damage-induced discontinuities in non-stationary signals. These studies leverage tools like wavelet transforms and hypothesis testing to process measured data but did not apply the Neyman-Pearson theorem to detection impulses.

Data from a Tainter valve operated by the U.S. Army Corps of Engineers is used to demonstrate the binary hypothesis testing framework. Sensors on the valve system detected acceleration impulses that aligned with irregular inclinometer readings on the sector gear. Likely caused by stick-slip behavior, these anomalies underscore the need for robust detection methods. This study applies the Neyman-Pearson theorem to detect such impulses in acceleration signals [12].

The remainder of this paper is organized as follows: Section 2 introduces the Tainter valve system, instrumentation, and data collection process. Section 3 presents observed impulses in acceleration signals alongside angular displacement anomalies. Section 4 discusses detection results using the Neyman-Pearson detection model. Finally, Section 5 summarizes the findings and conclusions.

DESCRIPTION OF THE TAINTER VALVE, INTRUMENTATION AND DATA COLLECTION

The Tainter valve mechanical system, operated by the U.S. Army Corps of Engineers, is a vital component of inland waterway infrastructure that supports both commerce and recreation. The valves are actuated by machinery mounted on the lock wall (Figure 1), including a gear train driven by a 40 horsepower, 4-pole, 480 volt three-phase induction motor powered by an inverter-fed variable frequency drive (VFD). This motor generates a rotating magnetic field in the stator, inducing rotor current that lags behind the synchronous speed. The VFD enables precise control of speed and voltage, operating mainly at 300 and 1800 revolutions per minute (RPM). The gear train rotates a shaft with a strut arm connected to the valve, raising or lowering it based on lock operation needs. Valve movement follows a controlled speed profile: during opening, the motor ramps from 0 to 300 RPM, holds until the valve reaches 12 inches, then accelerates to 1800 RPM and gradually stops over 6 seconds. The entire cycle takes about 5 minutes, with the closing cycle following the same pattern in reverse.

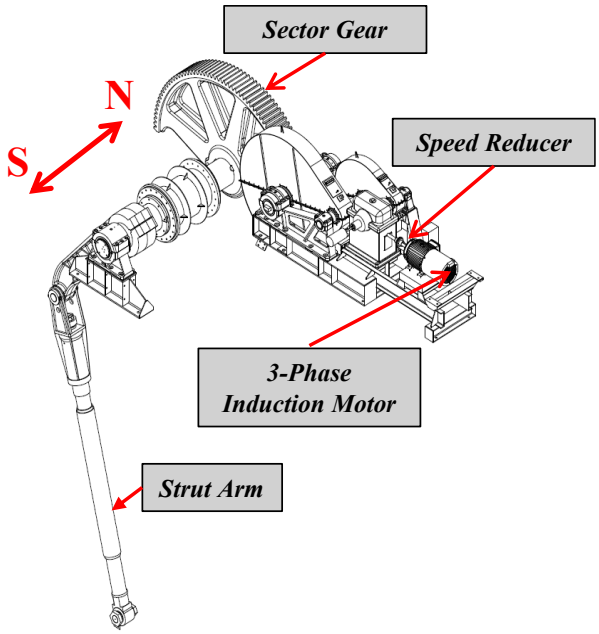

Figure 1 perspective view of the Tainter valve machinery system, including the key components: sector gear, speed reducer, 3-phase induction motor, and strut arm.

In Figure 2, sensors were strategically positioned to capture the mechanical and electrical behavior of the Tainter valve machinery. Four shear-mode ceramic ICP accelerometers (PCB Piezotronics 355B03) with a sensitivity of 100 mV/g, a measurement range of 100 g peak-peak, and a frequency range of 1 Hz to 10 kHz were mounted along the load path, including the motor, speed reducer, jack shaft, and sector gear bearing blocks, to monitor vibrations and detect mechanical irregularities. Each accelerometer was connected via a 50-foot coaxial cable with a 10-32 plug and BNC connector for reliable data transmission. A single-axis MEMS inclinometer from Jewell Instruments was magnetically mounted on the sector gear, outputting a 4-20 mA DC current proportional to the angular position with a resolution of approximately 0.05 degrees over its 180-degree range.

Sensors in the motor control center (MCC) and mechanical rooms are connected to a data acquisition (DAQ) system via ceiling-mounted cable trays. The DAQ enclosure includes a 6-slot United Electronic Industries (UEI) PowerPC Cube with an onboard field-programmable gate array (FPGA) and four mixed-signal input/output boards: AI211 (accelerometers), AI212 (thermocouples), AI217 (current transformers and inclinometer), and AI224 (strain gauges). An industrial Ethernet cable links the DAQ to a National Electrical Manufacturers Association (NEMA) enclosure in the MCC room containing a computer and external hard drive. Custom Windows Presentation Foundation (WPF) software manages data collection with a first-in, first-out buffer to

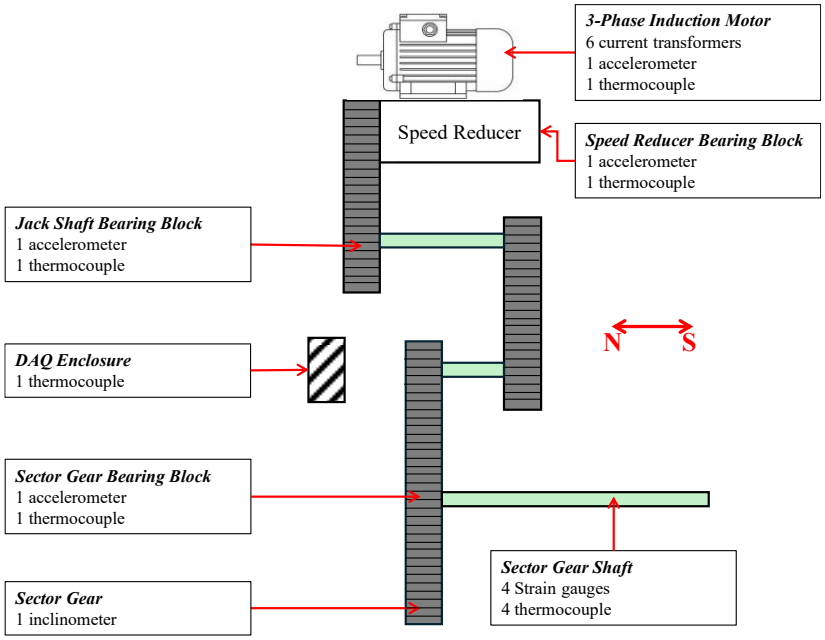

Figure 2 Layout of the instrumentation and key components of the Tainter valve machinery system, highlighting sensor placements and structural elements.

prevent loss, saving data in a structured format, with each board storing 30 days of per-second binary data. The AI211 board, which handles four accelerometers, samples vibration at 10 kHz per channel. Each is set for ±50 g range, 100 mV/g sensitivity, 5 mA excitation, and AC coupling. It uses four 24-bit oversampled A/D converters with over 109 dB dynamic range, synced to a clock running at eight times the sampling rate.

To reduce aliasing, onboard analog and digital filters are applied before down-sampling to the desired output rate.

OBSERVATION OF IMPULSES IN ACCELERATION DATA AND BUMPS IN INCLINOMETER DATA

Between May and November 2024, the valve's operations—including opening and closing—were managed based on waterway traffic. The degree to which the valve opened varied depending on the size and type of boats passing through. Figure 3 presents the recorded acceleration time histories for the motor, speed reducer, jack shaft, and sector gear bearing blocks, along with the angular displacement time history of the sector gear during a valve opening that occurred on May 21, 2024. During this event, the sector gear rotated clockwise from $82.39°$ to $-47.43°$. The opening process is divided into four distinct phases: (1) from 0.00 to 10.08 seconds, the valve remained closed, and the sector gear was stationary; (2) between 10.08 and 161.88 seconds, the valve began opening slowly; (3) from 161.88 to 289.83 seconds, the valve opened more rapidly; and (4) finally, from 289.83 to 297.00 seconds, the valve was fully open and the sector gear stopped moving. The slope of the angular displacement in Figure 3 (b) during different intervals reflects the rotational speed of the sector gear. Both the acceleration levels—excluding those at the sector gear bearing block—and the angular displacement slope were noticeably higher in Phase 3 compared to Phase 2.

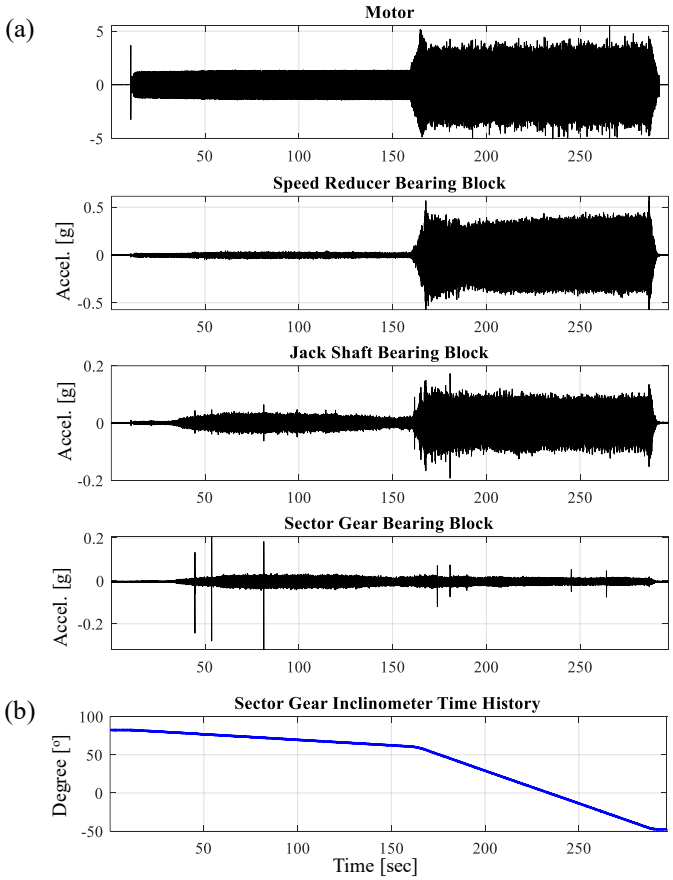

Figure 3 During a valve opening event: (a) measured acceleration time histories for the motor, speed reducer bearing block, jack shaft bearing block, and sector gear bearing block; and (b) measured angular displacement time history of the sector gear.

During Phases 2 and 3, acceleration data from the jack shaft and sector gear bearing blocks showed some impulses. Some impulses appeared in both channels at the same time, while others—such as those at 245.37 and 264.09 seconds in the jack shaft bearing block—did not align with any impulses in the sector gear bearing block. However, the presence of simultaneous impulses does not necessarily imply a causal connection. Furthermore, impulses were more frequent in Phase 2 (slow valve movement) than in Phase 3 (faster valve movement).

SINGLE-CHANNEL NEYMAN-PEARSON DETECTION RESULTS

In the Neyman-Pearson framework for binary hypothesis testing, the null hypothesis (H_0) and the alternative hypothesis (H_1) are defined as:

$$\begin{aligned} H_0 &: x = w \\ H_1 &: x = A + w \end{aligned}. \tag{1}$$

Here, x represents the measured acceleration signal from the sector gear bearing block, w denotes the noise component, and A is the deterministic impulse being targeted for detection. The noise is assumed to follow a Gaussian distribution, $w \sim N\left(0, \sigma^2\right)$. Based on this, the probability distributions of x under each hypothesis are as follows:

$$\begin{aligned} x; H_0 &\sim N\left(0, \sigma^2\right) \\ x; H_1 &\sim N\left(A, \sigma^2\right) \end{aligned}. \tag{2}$$

In binary hypothesis testing, two types of errors can occur: Type I (false positive) and Type II (false negative). A Type I error happens when the detector mistakenly identifies an impulse (A) in the measured signal (x) when none exists. A Type II error occurs when the detector misses the impulse even though it is present. These are quantified by the probability of false alarm (p_{FA}) and probability of detection (p_D), respectively.

Neyman-Pearson detection designs an optimal detector by fixing the false alarm probability (p_{FA}) to a predefined threshold while maximizing the detection probability (p_D). For a given p_{FA}, p_D is maximized by selecting the alternative hypothesis (H_1) when the following condition is satisfied:

$$\Omega_x : L(x) = \frac{p(x; H_1)}{p(x; H_0)} > \gamma . \tag{3}$$

Here, γ is the decision threshold, Ω_x denotes the detector operating in the x-domain, and $L(x)$ is the likelihood ratio comparing H_1 and H_0. Since positive impulses are the focus, A is assumed to be positive. By substituting the probability density functions for both hypotheses and applying the logarithm to both sides, the detector x -domain can be reformulated as:

$$\frac{Ax}{\sigma^2} - \frac{A^2}{2\sigma^2} > \log \gamma . \tag{4}$$

The threshold γ can be set according to the specified allowable false alarm probability p_{FA}, using the integral of the signal model under the null hypothesis. Likewise, the detection probability (p_D) can be calculated from the integral of the model under the alternative hypothesis. Since the probability density functions for both H_0 and H_1 are known (as given in Eq. (2)), the Neyman-Pearson detector and p_D be explicitly determined as follows:

$$x > \sqrt{2}\sigma \operatorname{erfc}^{-1}(2p_{FA})$$
$$p_D = \frac{1}{2}\operatorname{erfc}\left(\operatorname{erfc}^{-1}(2p_{FA}) - \frac{A}{\sqrt{2}\sigma}\right). \quad (5)$$

Here, $\operatorname{erfc}(\bullet)$ is the complementary error function, and $\operatorname{erfc}^{-1}(\bullet)$ denotes its inverse. The detector does not depend on the specific impulse; instead, it is determined by the false alarm probability (p_{FA}) and the noise standard deviation (σ). For a given p_{FA}, the probability detection (p_D) depends only on the SNR, defined as A/σ.

This section analyzes the acceleration signal from the sector gear bearing block (Figure 3), divided into successive 1-second segments. Figure 4(a) and (b) show the detected positive impulses and their corresponding thresholds for each window over the full acceleration time history, using $p_{FA} = 1\times10^{-5}$ and 1×10^{-6}, respectively. As expected, a higher p_{FA} leads to more detected impulses, while a lower p_{FA} results in fewer detections. For a 297-second acceleration record sampled at 1×10^{4} Hz, with a total of 2.97×10^{6} samples, a signal containing only noise would yield approximately 29.7 false detections with $p_{FA} = 1\times10^{-5}$, and about 2.9 with $p_{FA} = 1\times10^{-6}$. This underscores the importance of selecting p_{FA} based on the number of samples, as the test is applied to each sample individually. Moreover, choosing a small p_{FA} is essential when aiming to detect only genuine impulses. Figure 4 (c) presents the Receiver Operating Characteristic (ROC) curves under the Neyman-Pearson detection model for various SNR levels. As p_{FA} increases, the probability of detection also improves. Notably, when the SNR is low (e.g., $p_{FA} < 0.01$), p_D is highly sensitive to the predefined p_{FA}. Overall, the performance of the Neyman-Pearson detector improves significantly with higher SNR.

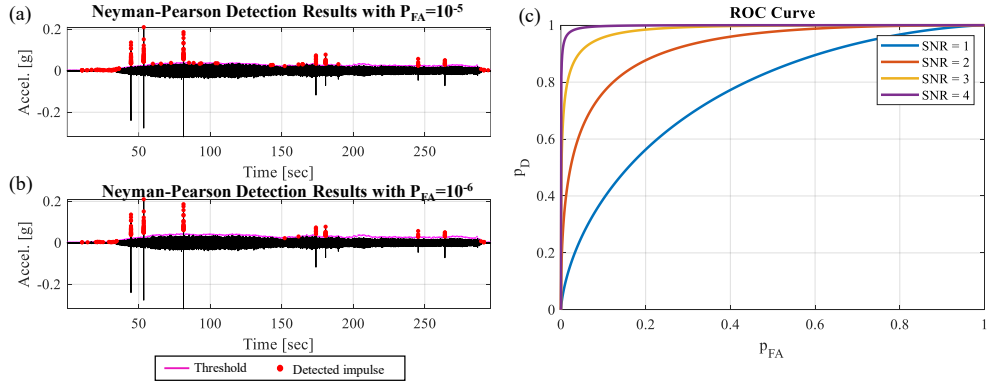

Figure 4 Single-channel Neyman-Pearson detection results for positive impulses: (a) $p_{FA}=1\times10^{-5}$; (b) $p_{FA}=1\times10^{-6}$; (c) ROC curve.

CONCLUSIONS

This study applies a Neyman-Pearson detection framework to a Tainter valve mechanical system. The system is instrumented with various sensors—current transformers, accelerometers, inclinometers, and thermocouples—covering components from the motor to the final gear shaft. During valve opening, consistent impulses appear in the acceleration signals at the jack shaft and sector gear bearing blocks, coinciding with excursions in the sector gear's angular displacement. These anomalies are suspected to be related to stick-slip behavior, though their exact source is unknown.

The paper focuses on detecting these impulses using binary hypothesis testing. A major challenge is the non-stationary nature of the acceleration signal. Neyman-Pearson hypothesis testing is applied to the acceleration data from the sector gear bearing block, using a null hypothesis (H_0) that the signal contains only noise, and an alternative hypothesis (H_1) that it contains both noise and impulses. The noise is assumed to follow a Gaussian distribution. Detection performance is evaluated using the probability of false alarm (p_{FA}) and probability of detection (p_D), representing Type I and Type II errors.

In this framework, impulses are treated as deterministic. For positive impulses, p_{FA} and p_D can be derived analytically. Due to the high sampling rate (10 kHz), p_{FA} must be very small to avoid false detections. The Neyman-Pearson detector successfully identifies clear positive impulses in the acceleration data. ROC curve analysis shows that detection performance improves as the assumed impulse magnitude increases. This study establishes a strong foundation for developing future detection frameworks that incorporate uncertainty in impulse characterization.

REFERENCES

1. Li, Y., B. Li, J. Ji, and H. Kalhori. 2022. "Advanced Fault Diagnosis and Health Monitoring Techniques for Complex Engineering Systems," *Sensors*, 22:10002. https://doi.org/10.3390/s222410002.
2. Sivasuriyan, A., D. S. Vijayan, P. Devarajan, A. Stefańska, S. Dixit, A. Podlasek, W. Sitek, and E. Koda. 2024. "Emerging Trends in the Integration of Smart Sensor Technologies in Structural Health Monitoring: A Contemporary Perspective," Sensors, 24:8161. https://doi.org/10.3390/s24248161.
3. Tagawa, Y., R. Maskeliūnas, and R. Damaševičius. 2021. "Acoustic Anomaly Detection of Mechanical Failures in Noisy Real-Life Factory Environments," *Electronics (Basel)*, 10:2329. https://doi.org/10.3390/electronics10192329.
4. Sun, L., J. P. Conte, M. D. Todd, et al. 2024. "Linear System Identification of the UC San Diego Geisel Library Building under Ambient Vibration," *J. Civ. Struct. Health Monit.* https://doi.org/10.1007/s13349-024-00889-4.
5. Sun, L., J. P. Conte, M. D. Todd, et al. 2023. "Linear System Identification of the UC San Diego Geisel Library Building," in *Proceedings*, pp. 61–70. https://doi.org/10.1007/978-3-031-39117-0_7.
6. Eick, B., B. Kim, K. Atwater, and B. Spencer. 2024. "Self-Excited Hoisting Chain Tension Measurements for Dam Spillway Gates and Identification of Uneven Hoisting," *J. Civ. Struct. Health Monit.* https://doi.org/10.1007/s13349-024-00866-x.
7. American Society of Civil Engineers. n.d. *2021 Report Card for America's Infrastructure*. https://infrastructurereportcard.org/.

8. Liu, J., Y. Sha, W. Zhang, et al. 2024. “Anomaly Detection Method for Industrial Control System Operation Data Based on Time–Frequency Fusion Feature Attention Encoding,” *Sensors*, 24:6131. https://doi.org/10.3390/s24186131.
9. Wee, A., D. B. Grayden, Y. Zhu, et al. 2008. “A Continuous Wavelet Transform Algorithm for Peak Detection,” Electrophoresis, 29:4215–4225. https://doi.org/10.1002/elps.200800096.
10. An, G., Z. Huang, and Y. Li. 2023. “Constant False Alarm Rate Detection of Pipeline Leakage Based on Acoustic Sensors,” *Sci. Rep.*, 13:14149. https://doi.org/10.1038/s41598-023-41177-3.
11. Robertson, A. N., C. R. Farrar, and H. Sohn. 2003. “Singularity Detection for Structural Health Monitoring Using Hölder Exponents,” *Mech. Syst. Signal Process.*, 17:1163–1184. https://doi.org/10.1006/mssp.2002.1569.
12. Kay, S. 1998. *Fundamentals of Statistical Signal Processing: Detection Theory*. Upper Saddle River, NJ: Prentice Hall.